Pergamon

Int. J. Heat Mass Transfer. Vol. 41, No. 13, pp. 2037–2047, 1998

Printed in Great Britain
0017–9310/98 $19.00+0.00

PII: S0017–9310(97)00227–5

The geometric optics approximation for reflection from two-dimensional random rough surfaces

KAKUEN TANG and RICHARD O. BUCKIUS†

Department of Mechanical and Industrial Engineering, University of Illinois at Urbana-Champaign, 1206 West Green, Urbana, IL, 61801, U.S.A.

(*Received* 10 *February* 1997 *and in final form* 31 *July* 1997)

Abstract—The geometric optics approximation for wave scattering from two-dimensional random rough surfaces is compared to the experimental results from five independent facilities and to the existing numerical electromagnetic theory predictions. The samples include both metallic and dielectric materials with surface slopes ranging from 0.11–0.71. The surface roughness and incident wavelength vary from 0.57–3.58 and from 0.64 microns–3.00 millimeters, respectively. The geometric optics results are in good agreement with all the electromagnetic theory calculations and the experimental findings for the considered two-dimensional surfaces. In addition, the two-dimensional geometric optics approximation predicts both the phenomenon of retro-reflection for surfaces with a slope as low as 0.33 and off-specular peak reflection. For surface parameters within the geometric optics domain of validity for one-dimensional random rough surfaces, the geometric optics results indicate that the one-dimensional domain is valid for two-dimensional surfaces.

INTRODUCTION

Wave scattering from interfaces is important in various science and engineering disciplines including photorealistic image generation in computer graphics; radio and sound wave scattering from ocean surfaces, atmospheric layers and planets in communication; image pattern analysis in surface contamination detection; specularity prediction in spacecraft design; emittance estimation in furnace design; and reflection determination in optical instruments. However, the ability to predict such realistic surface scattering from very rough surfaces through rigorous theory has only recently been developed, and results are only available in a few limited cases. Extensive rigorous predictions for random rough surfaces with dielectric properties and relative rough surface slopes are still required. As compared to rigorous two-dimensional surface scattering approaches, approximate models for two-dimensional scattering and exact results for one-dimensional surfaces have received considerable attention, yet their application to more general two-dimensional surfaces still requires further investigation. Thus, there is the need to develop methods to accurately predict the scattering from very rough two-dimensional surfaces and to quantify the accuracy of the methods.

Analytical investigations of surface scattering can be classified into two broad categories: exact methods derived from electromagnetic theory and approximate models developed through simplifications. Exact approaches are typically based on the extinction theorem and Green's theorem, without restrictions on material properties or geometric parameters including correlation length, τ, and surface roughness, σ. Thus, exact solutions can be applied to the scattering problems with surface geometric parameters on the order of the incident wavelength, λ. However, due to the computational limitations, predictions are typically for one-dimensional surfaces, with few studies on two-dimensional samples. One-dimensional exact approaches have been successfully applied to dielectric, metallic or perfectly conducting surfaces [1–7], deterministic surfaces [8, 9], thin metal films [10], dielectric films on a glass substrate [11] and free-standing dielectric films [12]. Such exact calculations have been compared with experimental findings [11–14] and with approximate models [2, 7, 15, 16]. Few two-dimensional exact solutions have been reported [17–23]. Most solutions consider perfectly conducting surfaces with only one investigation on a metallic surface. Also, in most of these studies, surface slope (represented by σ/τ) is less than unity and incident angle is less than 30°. These approaches are generally based on Monte Carlo simulations together with certain iteration schemes.

Exact approaches to wave scattering are very computationally intensive, typically involving the solution of multiple coupled integral equations. This is especially true for random rough surfaces in which the reflection distribution has to be averaged over numerous realizations. In general, for two-dimen-

† Author to whom correspondence should be addressed.

NOMENCLATURE

I	intensity
$\mathbf{n}$	surface outward normal vector
$\mathbf{r}$	position vector
$\mathbf{V}_0$	incident vector
$\mathbf{V}_s$	reflected vector
x, y, z	surface coordinates.

Greek symbols

ζ	surface profile
θ	polar angle
λ	wavelength
ρ'', ρ'	bi-directional reflection function, hemispherical reflectivity
σ	standard deviation
τ	surface correlation length
ϕ	azimuthal angle
Φ	radiant power flow
Ω	solid angle.

Subscripts

0	incident
s	scattered
x, y, z	coordinates.

Superscript

$''$	bi-directional.

sional surfaces, the required CPU times are more than an hour per realization (for machines equivalent to the Cray C90), and the number of surface field unknowns is of the order of hundreds of thousands. To circumvent these difficulties, various surface scattering approximations have been developed. Specular (Fresnel) and diffuse (Lambertian) models are two of the often-used approximations. In the specular model, energy is reflected in the solid angle region around the specular angle ($\theta_s = \theta_0$) and the fraction of the reflected energy is found with Fresnel relations. In the diffuse model, energy is assumed to be equally distributed in all directions and the bi-directional reflectivity is simply calculated by the cosine law.

The Kirchhoff approximation [24], unlike Fresnel and Lambertian approximations in which neither surface parameters nor incident wavelength are directly involved, provides reflection distributions between the specular and the diffuse reflection models. The reflected magnetic and electric fields on each point on the surface are approximated by the field that would exist on a tangent plane to the surface at this point. The Kirchhoff approximation has been applied to both one-dimensional and two-dimensional random rough surfaces and domains of validity have been constructed [2, 15, 25, 26]. It is commonly believed that the Kirchhoff approximation yields an accurate solution when surface geometric parameters are comparable with the incident wavelength and the surface slope is less than 0.3. Many improvements and extensions [27–30] of the Kirchhoff approximation, resulting in an enlarged domain of validity, have been reported.

The geometric optics approximation also termed ray tracing, tracks the energy throughout its interaction with the surface until it leaves the surface. It is commonly believed that this approximation is accurate if both normalized correlation length, τ/λ, and normalized surface roughness, σ/λ, are greater than unity. Actually, Tang *et al.* [16] have demonstrated that the one-dimensional geometric optics approximation can yield an accurate solution even when both surface parameters are less than unity. The angular nature of the geometric optics approximation results are compared with exact solutions obtained by the integral equation method [3, 8]. With a directional criterion, the approximation can be applied for surfaces as rough as $\sigma/\tau = 4.0$, providing $\sigma/[\lambda\cos(\theta_0)]$ is greater than 0.17.

Various experimental results have been obtained to quantify scattering phenomena, and most results focus on in-plane reflection measurements from two-dimensional surfaces. Torrance and Sparrow [31] experimentally studied the off-specular peak phenomenon in which the maximum reflected intensity occurs at angles other than the specular angle, $\theta_s = \theta_0$. In their study, the off-specular peaks occur at angles greater than specular angles. The basic experimental parameters were systematically varied with the incident and reflected angles between 10–75° and 0–89°, respectively. The incident and reflected solid angles were estimated to be 0.0035 steradians. The energy sources were globar rod and fluorescent bulb, providing incident wavelength in the infrared and visible regions. The rough samples included both metals (nickel, copper and nickel–copper alloy) and dielectric materials (magnesium-oxide ceramic and aluminum oxide) with roughness varying from 0.23–5.80 μm. The surface roughness was measured by a profilemeter with a diamond stylus of radius 1.26 μm. No correlation lengths of the samples were provided. Smith *et al.* [32] observed off-specular peak in which the maximum reflected intensity occurs at angles smaller than specular angles. This phenomenon occurs for dielectric materials if the surface roughness is significantly greater than the incident wavelength and the incident angle is greater than the Brewster angle. The experiments were conducted on glass surfaces with a refractive index of approximately 1.50 and the surface roughness ranged from 0.34–5.22 μm. Simi-

larly, no correlation lengths were given except for a case. The incident and reflected angles varied from 0–76° and 0–90°, respectively. While the reflected angle increment was generally 5°, a smaller increment was used around the maxima. All measurements were for an incident wavelength of 0.5 μm. The reflection results from both of these studies were presented in the normalized form.

Ford *et al.* [33] employed a Fourier transform infrared system for bi-directional reflection measurements which provides the reflection response at multiple wavelengths. Reflection measurements have been reported for a random rough gold-coated sample with $\sigma/\tau = 0.19$ and $\sigma/\lambda = 2.3$, and the maximum of each reflection distribution occurs slightly beyond the specular angle, $\theta_s = \theta_0$. Experimental results are compared with exact solutions obtained from a one-dimensional integral equation approach [3, 8]. The experimental and theoretical predictions are in good agreement in the reflection distribution but the magnitude of the bi-directional reflectivity for a random rough gold-coated surface is significantly lower than the exact solutions since the theoretical predictions are based on a one-dimensional surface model. Similar studies on other samples such as gold sandpapers and aluminum alloys have also shown the off-specular peak phenomena for thermal radiation [34–37].

The phenomenon of retro-reflection (energy is reflected back in the incident solid angle region, $\theta_s = -\theta_0$) has been observed independently by different experimental investigators [11, 12, 38–40] which have a capability of reflection measurements at negative scattering angles. O'Donnell *et al.* [41] were among the first researchers to experimentally study retro-reflection from two-dimensional random rough surfaces. Three gold-coated samples were manufactured in a manner similar to the fabrication of integrated circuit devices [42] with $\sigma/\tau = 0.11$, 0.20 and 0.71. Strong retro-reflection peaks occur at anti-specular angles for the roughest sample at incident angles of 0, 20 and 40°. Chan *et al.* [43] has also reported similar observations. Their samples were machine-fabricated by specified two-dimensional random rough surface profiles, and layers of metallic paint were coated on the samples after fabrication. The ratio of roughness to correlation length ranged between 0.25 and 0.71. Measurements were made at reflected angles from −70–70° with incident wavelengths on the order of millimeters (~3 mm) and incident angles of 0, 20 and 40°. A slight retro-reflection peak was observed for the surface with a slope of 0.33, and the retro-reflection peak becomes more pronounced as surface slope increases to 0.71.

In this work, the geometric optics approximation on the electromagnetic theory is examined for two-dimensional random rough surfaces. The geometric optics approximation is presented and compared to the existing experimental results and electromagnetic theory calculations. Also, new experimental results are reported and compared to the geometric optics approximation. The following section defines the bi-directional reflectivity and two-dimensional random rough surfaces specifications and provides a detailed description of the geometric optics model. In the subsequent section, approximate results are compared with the experimental findings from five facilities and electromagnetic theory calculations.

GEOMETRIC OPTICS SCATTERING ANALYSIS

Bi-directional reflectivity

When a semi-transparent surface is illuminated by an electromagnetic wave, the incident energy will be reflected and transmitted. To describe the angular distribution of the reflected energy, the bi-directional reflectivity is defined as π times the ratio of the reflected power per unit solid angle per unit projected area to the incident power [44] and given as

$$\rho''_\lambda(\Omega_0, \Omega_s) = \frac{\pi \dfrac{d\Phi_s}{d\Omega_s}}{\cos(\theta_s)\dfrac{d\Phi_0}{d\Omega_0}} \tag{1}$$

where Φ and Ω are the radiant power and solid angle, the subscripts 0 and s denote incident and scattering, respectively. Note that the bi-directional reflectivity can be greater than unity. Integrating the bi-directional reflectivity over the entire hemisphere and dividing the π yields the directional reflectivity (the ratio of the total hemispherical reflected power to the total hemispherical incident power). For a perfectly conducting surface (no energy absorption or transmission), the directional reflectivity is unity.

Two-dimensional random rough surfaces

Two-dimensional random rough surfaces are generated by a stationary stochastic process with a zero mean and a Gaussian probability density function of the surface height [43], $\zeta(\mathbf{r})$. Thus,

$$\langle \zeta(\mathbf{r}) \rangle = 0 \tag{2}$$

$$\langle \zeta(\mathbf{r}_1)\zeta(\mathbf{r}_2) \rangle = \sigma^2 \exp\left[-\left(\frac{|x_1 - x_2|^2}{\tau_x^2} + \frac{|y_1 - y_2|^2}{\tau_y^2} \right) \right] \tag{3}$$

where $\mathbf{r}$ is the position vector and x, y are the components of $\mathbf{r}$. The subscripts 1 and 2 denote two different locations on the surface. τ_x and τ_y are the correlation lengths in x and y dimensions, and σ is the surface roughness. In this work, surfaces are assumed to be isotropic, exhibiting no preferential roughness direction; thus τ_x and τ_y are equal and denoted by τ.

Figures 1(a) and (b) show realizations of two-dimensional random rough surfaces with surface parameters of $\tau_x/\lambda = \tau_y/\lambda = \tau/\lambda = 2.0$ and $\sigma/\lambda = 0.2$, and $\tau_x/\lambda = \tau_y/\lambda = \tau/\lambda = 1.0$ and $\sigma/\lambda = 0.7$, resulting surface slopes of 0.1 and 0.7, respectively. The horizontal axes are x/λ and y/λ, while the vertical axis is ζ/λ.

These two surface profiles represent surfaces that exhibit both specular and diffuse scattering characteristics.

Two-dimensional geometric optics approximation

The geometric optics approximation to electromagnetic theory provides a multiple scattering solution for surface reflection. In this approximation the energy incident on a rough surface is traced through multiple interactions with the surface until it leaves the surface, and Fresnel reflection is applied to each local point of intersection. For a rough surface, the number of interactions typically increases with surface slope. For a plane surface, the geometric optics approximation reduces to the Fresnel reflection since all the energy is reflected in the solid angle region around the specular angle.

The first step of the two-dimensional geometric optics approximation is to generate a random rough surface profile and its directional slopes for the pre-specified correlation length, surface roughness, incident wavelength, dielectric constants and surface length. The first reflection points [see Fig. 2(a), point A] are chosen from either randomly distributed or equally spaced points in both x and y dimensions. Since both schemes provide the same results, and since the latter takes less computational time, equally spaced points are selected. The first reflection point may not necessarily be a node; thus, there can be more first reflection points than nodes. In order to obtain accurate results, the number of first reflection points should be five times greater than the number of nodes.

The direction of the incident bundle is pre-specified and expressed in a vector, $\mathbf{V}_0 = x\mathbf{i}+y\mathbf{j}+z\mathbf{k}$, where $x = \sin(\phi_0)\cos(\theta_0)$, $y = \sin(\phi_0)\sin(\theta_0)$ and $z = \cos(\phi_0)$. As illustrated in Fig. 2(b), some surface elements [e.g., point C in Fig. 2(b)] do not participate in the scattering process since the incident bundle cannot hit portions of the surface. This shadowing contribution is significant at large θ_0. To determine if the first reflection point is in the shadow, the plane formed by the incident bundle direction and the projected line of the incident beam on the xy plane is considered. If any surface point between the first reflection point and the highest surface point in this plane lies above the incident bundle, the first reflection point is in a shadow, and another first reflection point is selected. If the bundle strikes the surface, the direction of reflection, $\mathbf{V}_s$, is found by using Snell's Law [45] in which the angle between the incident and normal vectors is equal to the angle between the reflected and normal vectors,

$$\mathbf{V}_s = \mathbf{V}_0 + 2|\mathbf{V}_0 \cdot \mathbf{n}|\mathbf{n} \tag{4}$$

where $\mathbf{n}$ is the normal vector. The energy carried by the bundle is equal to the projected area of the surface on the plane which has a normal parallel to the incident vector, $\mathbf{V}_0$.

Determining whether the reflected bundle strikes the surface again requires the same process as determining whether the first reflection lies in a shadow except that the direction in Fig. 2(b) is reversed, and the plane formed by the reflected bundle direction and its projected line on the x–y plane are considered. If any one of the points between the reflection point and the highest surface point in this plane lies above the bundle, the bundle restrikes the surface. If the highest point on the projected line is examined and the bundle does not restrike the surface, the reflected bundle is considered scattered from the surface. In addition, when the reflected bundle travels beyond the edges of the surface without striking the surface, the surface nodes are mirror-imaged on the opposite sides with the surface normal vector reversed.

After all of the bundles have been scattered from the surface for all first reflection points at a given incident angle, the bi-directional reflectivity is found from equation (1). The scattered energy is multiplied by π and divided by the total incident energy, the size of the solid angle and $\cos(\theta_0)$.

The numerical implementation of this process requires approximately 60 realizations to yield a statistically significant result. Surface length must be at least 50λ and at least 10 000 surface nodes are required to obtain an accurate result. Also, as the surface roughness increases, more surface nodes are needed for the surface. Numerical error in each realization is infinitesimal and the reported error is dependent upon the number of incident bundles, number of realizations and number of surface nodes. For the results presented in this work, this numerical error is less than 5.0%. The whole process for a surface with $\sigma/\tau < 0.25$, takes approximately 1 h of CPU time and 20 Megawords of memory on the Cray C90 to predict the averaged reflection distribution from 60 realizations. And for a very rough surface with $\sigma/\lambda > 0.7$, the prediction process takes about 5 h and 40 Megawords. These computations require approximately one-third of the CPU time and memory used for prediction of exact solutions on one-dimensional random rough surfaces.

EXPERIMENTAL MEASUREMENTS

A Fourier Transform Infrared Spectrometer (FTIR) [33, 46] coupled with a reflectometer is used for the in-plane bi-directional reflection measurements. This system simultaneously characterizes the reflection at multiple wavelengths simultaneously, and also has a capability for transmission and emission measurements for various interfaces. Results are reported here for reflection from rough gold-coated surfaces at 3.39 μm.

The basic elements of the system are a 1500 K air-cooled Ever-Glo™ source and a high-sensitivity liquid-nitrogen cooled mercury cadmium telluride detector (MCT) which provide an overall operating range from 1–16 μm. The linear region of the MCT

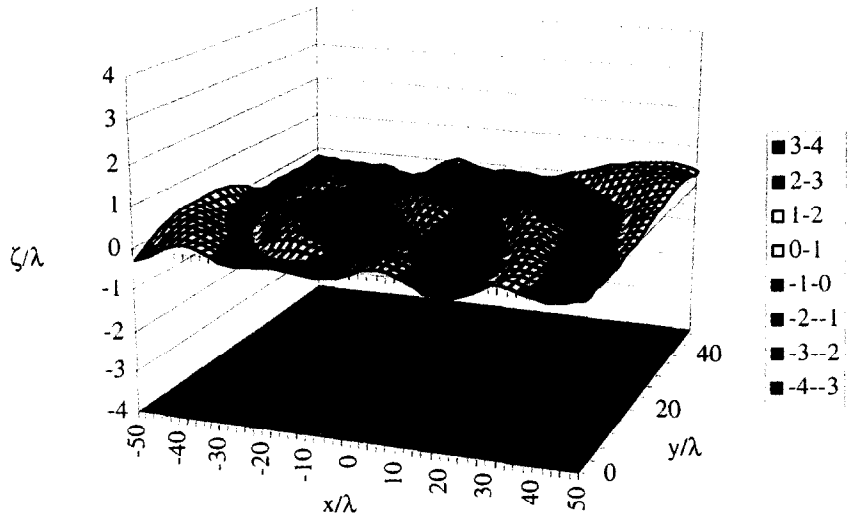

(a)

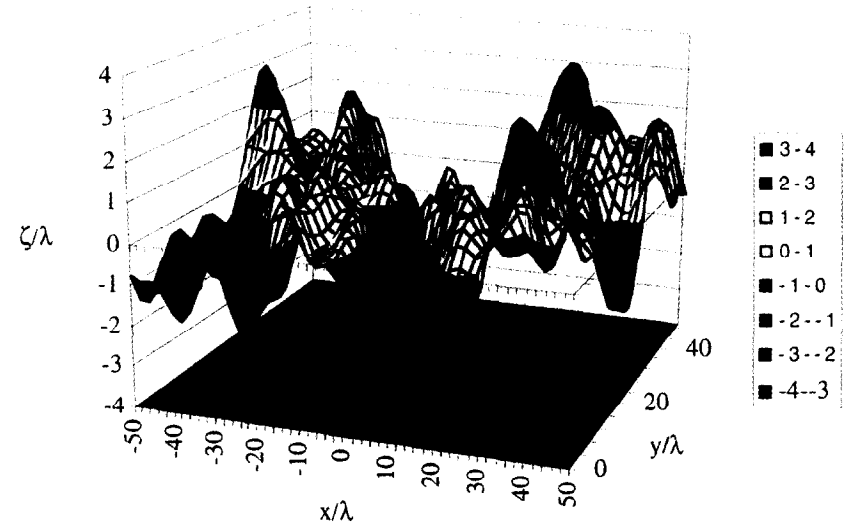

(b)

Fig. 1. Realization of surfaces: (a) $\sigma/\tau = 0.1$, $\sigma/\lambda = 0.2$ and (b) $\sigma/\tau = 0.7$, $\sigma/\lambda = 0.7$

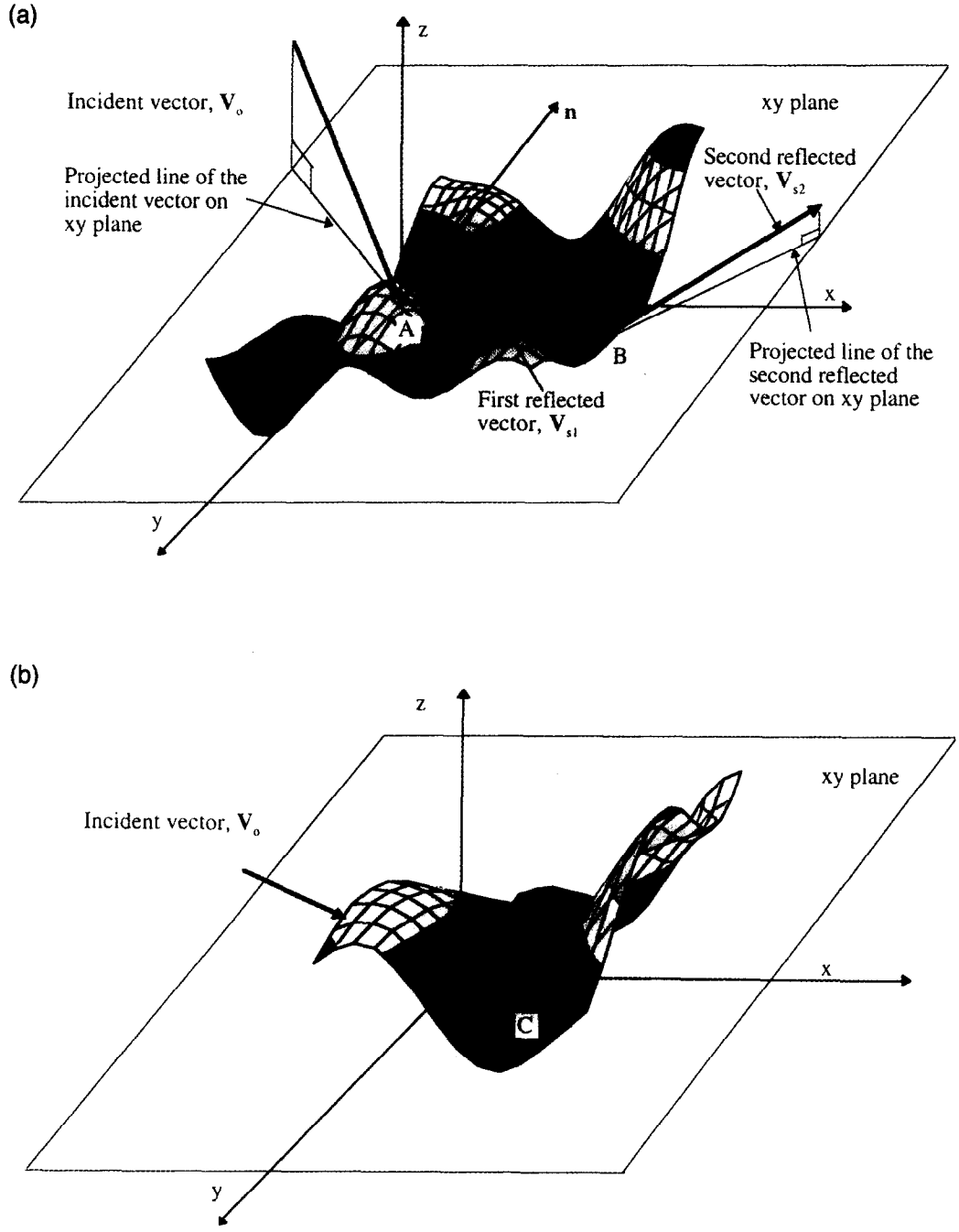

Fig. 2. (a) Rough surface scattering geometry. (b) The shadowing contribution.

detector is determined by recording signals for a blackbody radiation source and comparing the recording signals to the predicted values based on the Planck function [44]. The blackbody source intensity can be controlled by systematically varying exit aperture sizes and source temperatures. All the FTIR data presented in this work are within the linear region. Ellipsoidal and plane mirrors are installed in the reflectometer to provide an in-plane reflection measurement with variable incident and reflected angles. Several limiting apertures at the inlet and exit ports of the reflectometer, combined with the source aperture, provide the adjustment of incident and reflected solid angles which are set in a planar angle of approximately 4°.

The bi-directional reflectivity is determined by ratioing the measurements of the sample to a reference material. In this experiment, Spectralon (sintered polytetrafluoroethylene) designed by Labsphere, Inc. was chosen to be the reference material because of its repeatable, long term stability and diffuse reflectance properties. The bi-directional reflectivity of Spectralon was measured by TMA Technologies, Inc. [47]. As indicated in ref. [33], the overall uncertainty for the measured data is less than 10%.

Reflection measurements have been performed on two random rough gold-coated samples for various incident and scattering angles. The samples were manufactured by Labsphere, Inc. with surface geometric parameters $\sigma/\tau = 0.19$, $\sigma/\lambda = 2.30$ and $\sigma/\tau = 0.36$, $\sigma/\lambda = 7.24$ at the incident wavelength of 3.39 μm. Measurements of the geometric parameters for the smoother surface were conducted on a Dektak 3030 surface profilemeter, and the Dektak ^{3}st surface profilemeter was used to obtain the parameters for the rougher sample. The measured values are the ensemble average of 100 profiles randomly scanned on both samples. For the smoother surface, each scan length is 1000 μm, and each measured profile is represented by 400 grid points, while 2000 μm scan length and 2000 grid points are used for the rougher surface.

RESULTS AND COMPARISONS

In this section, the geometric optics predictions on two-dimensional surfaces are first compared to using the existing experimental findings. Figure 3 presents the normalized bi-directional reflectivity from the geometric optics approximation together with the existing experimental findings from four experimental facilities [31, 32, 41, 43]. The results are presented in ascending order of surface slope for curves (a) through (l). The results are shown in plane of incidence, $\phi_0 = 0°$. The vertical axis is the bi-directional reflectivity normalized with respect to its value at the specular angle [and multiplied by $\cos(\theta_s)$]. The geometric optics pre-

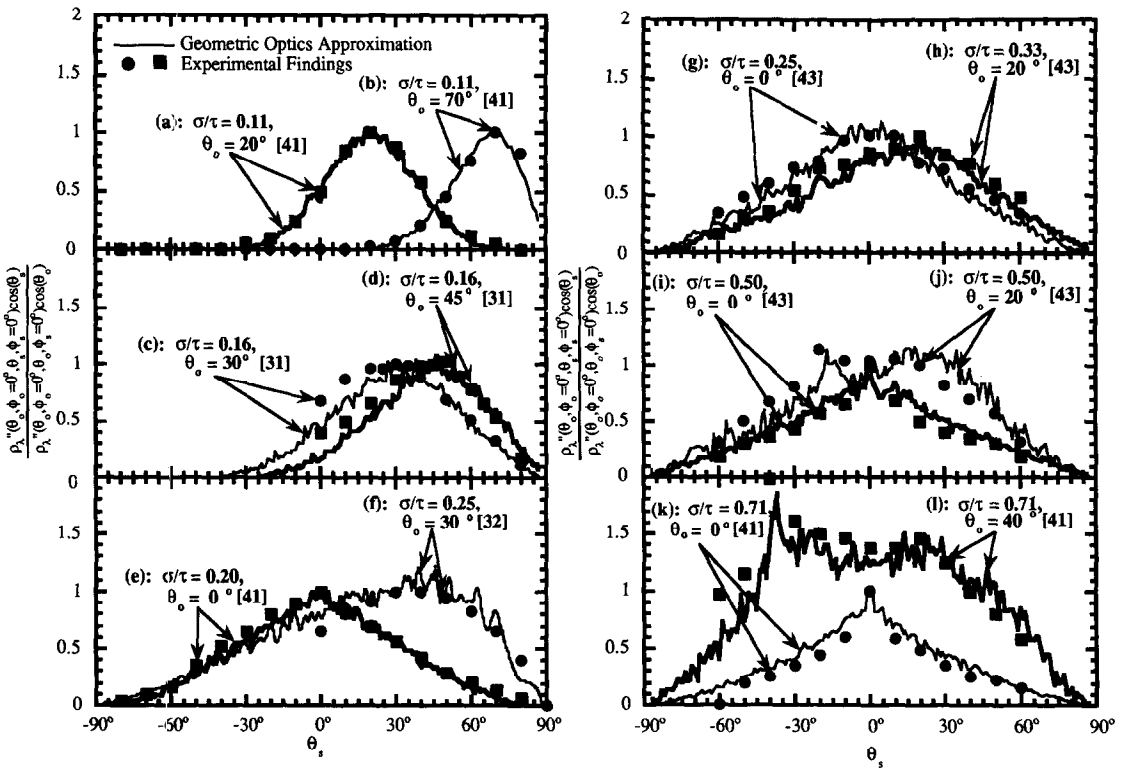

Fig. 3. Comparisons of geometric optics approximations with existing experimental findings for the normalized bi-directional reflectivity (see Table 1 for specific values of σ/λ).

Table 1. Surface parameters, surface materials, incident angles and incident wavelengths for the existing experimental findings presented in Fig. 3

Fig. 3 curve	Ref.	σ/τ	σ/λ	λ	θ_0	Materials
a	41	0.11	3.58	0.63 μm	20°	Gold
b	41	0.11	3.58	0.63 μm	70°	Gold
c	31	0.16	0.57	0.50 μm	30°	Aluminum
d	31	0.16	0.57	0.50 μm	45°	Aluminum
e	41	0.20	0.93	10.6 μm	0°	Gold
f	32	0.25	1.77	0.50 μm	30°	Glass
g	43	0.25	1.00	3.00 mm	0°	Perfectly conducting
h	43	0.33	1.00	3.00 mm	20°	Perfectly conducting
i	43	0.50	1.00	3.00 mm	0°	Perfectly conducting
j	43	0.50	1.00	3.00 mm	20°	Perfectly conducting
k	41	0.71	1.00	0.64 μm	0°	Gold
l	41	0.71	1.00	0.64 μm	40°	Gold

dictions are shown with solid lines and experimental findings with specific points. Complete listings of the surface roughness, correlation lengths, surface materials, incident angles and incident wavelengths of each case are indicated in Table 1.

Curves (a)–(e) in Fig. 3 illustrate the results from smaller roughness surfaces ($\sigma/\tau < 0.25$). Since the correlation lengths of the cases presented in curves (c) and (d) were not reported, the values of τ are selected as best fits to the experimental data as reported in ref. [30]. In these cases, both the geometric optics predictions and the experimental findings are Gaussian-shaped curves around the scattering angles, and the reflection distribution spans a limited range of scattering angles. No distinct off-specular peaks has been noticed in curves (a) and (b), while slight off-specular peaks occur in cases (c) and (d). In general, the geometric optics predictions are in excellent agreement with the experimental findings. Other researchers [30, 41] had compared these experimental findings with the other approximate predictions such as the Kirchhoff approximation, and the approximate approaches are in less accurate agreement in both trend and magnitude than the geometric optics results.

The results from surfaces with immediate roughness ($0.25 < \sigma/\tau < 0.70$) are presented in curves (f)–(j). The reflection distribution is no longer a Gaussian-shaped curve and the distribution spreads over the entire hemisphere. The agreement between the experimental findings and approximate results is excellent. An off-specular peak is also observed for the case (f). The maxima of the bi-directional reflectivity occurs at approximately $\theta_s = 35°$, instead of the specular angle, $\theta_s = 30°$. These results have also been compared with a single scattering model [32], with excellent agreement between the approximate prediction and experimental data at the small scattering angles ($\theta_s < 35°$); however, a significant direction between the single scattering model and experimental findings as θ_s increases was noted, indicating that the multiple scattering included here is important in cases where the surface slope is $\sigma/\tau \geqslant 0.25$.

A slight retro-reflection peak is observed at the anti-specular angle for both the geometric optics predictions and experimental findings in curve (h). This phenomenon is more distinct in the reflection distribution from the very rough surfaces as shown in curves (i)–(l). The distribution is very diffuse and large values of reflection are observed in the negative scattering angles. For the normal incidence [curves (i) and (k)], both experimental and approximate reflection distributions exhibit a strong single retro-reflection peak at normal scattering. At an incident angle of 40° [curve (l)], a sharp peak occurs at $\theta_s = -40°$ and a smaller forward peak occurs at $\theta_s = 20°$.

Other researchers [17–23] have predicted the reflection distribution for the cases (i) through (k) by electromagnetic theory simulations. In general, the results agree well except for the case (i) where a deviation in trend between the experimental results reported in ref. [43] and the electromagnetic theory calculations presented in ref. [17] is observed. Since good agreement between the experimental data reported in ref. [43] and other electromagnetic theory calculations [18, 20, 21] has been observed, comparisons with the electromagnetic theory predictions of refs. [18–21] are made rather than with ref. [17].

Figure 4 illustrates the absolute magnitude of the bi-directional reflectivity of gold-coated random rough surfaces, obtained from the FTIR system described in the previous section. The geometric optics predictions for both two-dimensional random rough surfaces and experimental results are presented at incident angles of 30, 35 and 45°, and at the incident wavelength of 3.39 μm. The results are in very good agreement in both trend and absolute magnitude. The large magnitude, limited scattering angle range and the Gaussian-shaped reflection distribution are observed for the smoother surface [curves (a)–(c)], while the rougher sample has a smaller magnitude, more diffuse and less-Gaussian shaped reflection distribution [curves (d)–(f)]. Off-specular peaks are observed for both surfaces. The maximum values of the reflection distribution occur at angles greater than the specular

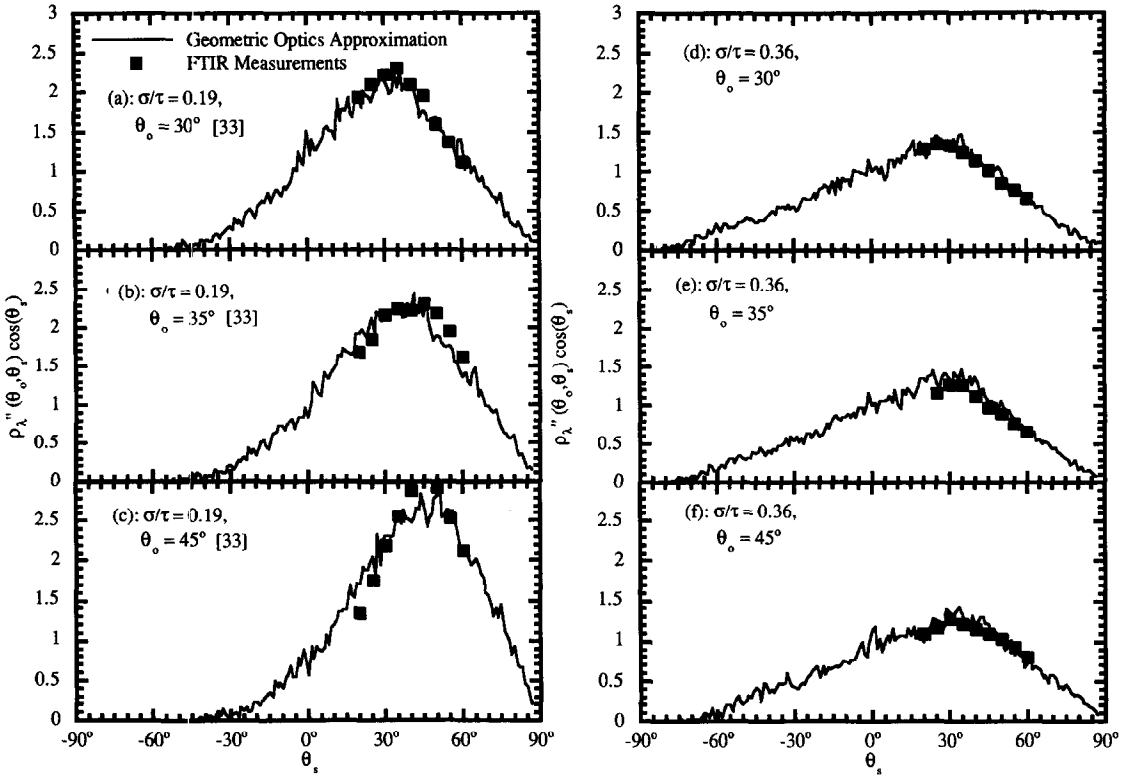

Fig. 4. Comparisons of geometric optics approximations with existing experimental findings for the bi-directional reflectivity from the gold-coated surfaces at a wavelength of 3.39 microns.

angles for the smoother surface, while for the rougher surface, the maximum values are at angles smaller than the specular angles. For the smoother surface, relative results were presented in ref. [33], and the trends predicted by a one-dimensional model were noted to be approximately 50% lower than exact solutions. The geometric optics results presented here indicate that the two-dimensional model is required for accurate absolute predictions of the bi-directional reflectivity from two-dimensional surfaces.

Geometric optics predictions are compared with electromagnetic theory calculations [19–21] in Fig. 5.Macaskill and Kachoyan [18] have compared electromagnetic theory calculations with some experimental findings presented in Fig. 3 [curves (k) and (l)]. In these cases, the comparisons of the geometric approximation to the electromagnetic theory calculations are not presented in Fig. 5. For these cases, the experimental findings agree well with electromagnetic theory calculations except no forward peak was observed because of the insufficient number of realizations. The results shown in Fig. 5 are presented in ascending order of surface slope for curves (a)–(d). Geometric parameters, surface materials, incident angles and wavelengths are listed in Table 2. The results are shown in the plane of incidence and compared to normalized electromagnetic theory calculations [19–21]. The geometric optics predictions

Table 2. Surface parameters, surface materials, incident angles and incident wavelengths for the existing electromagnetic theory calculations presented in Fig. 5

Fig. 5 curve	Ref.	σ/τ	σ/λ	θ_0	Materials
a	20	0.30	0.20	10°	Perfectly conducting
b	22	0.33	1.00	20°	Perfectly conducting
c	19	0.71	0.50	20°	Perfectly conducting
d	22	0.71	1.00	20°	Perfectly conducting

and electromagnetic theory calculation are found to be very similar for all scattering angles. Retro-reflection peaks are observed in anti-specular angles.

The good agreement between the geometric optics approximation and both existing experimental and rigorous electromagnetic theory predictions indicates that the geometric optics model provides a useful and relatively inexpensive approach for two-dimensional random rough surfaces with various slope surfaces σ/τ even beyond 0.3 (the limitation of the Kirchhoff approximation). Also the comparisons indicate that the geometric optics approximation has the capability to accurately predict retro-reflection peaks and off-specular peaks for random rough surfaces.

Although electromagnetic theory calculations pro-

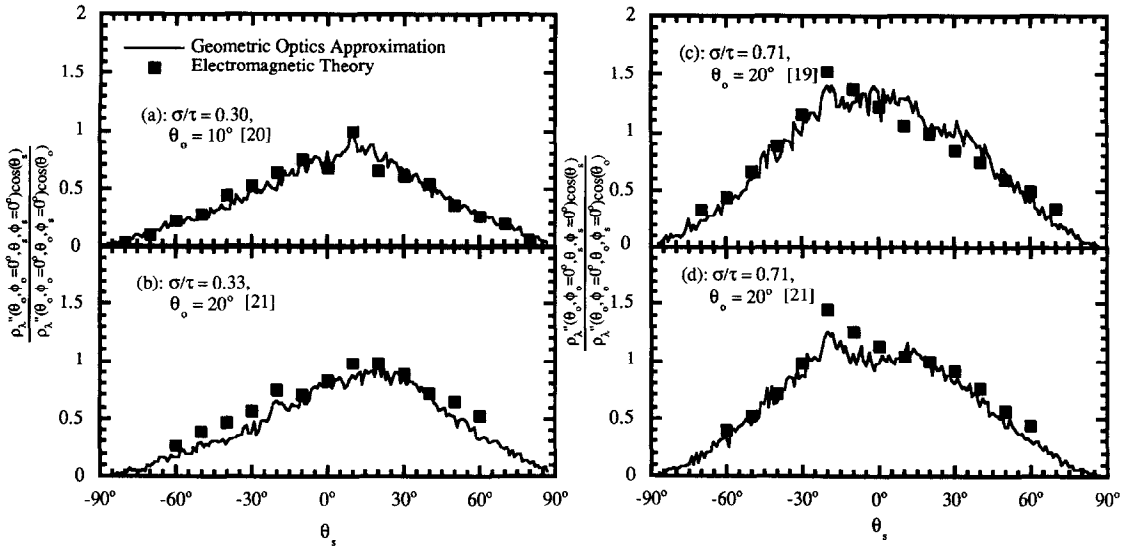

Fig. 5. Comparisons of geometric optics approximations with existing electromagnetic theory calculations for the normalized bi-directional reflectivity (see Table 2 for specific values of σ/λ).

vide an accurate means for the quantification of two-dimensional surface reflection, such investigations are expensive and limited; thus, constructing a comprehensive domain of validity of the two-dimensional geometric optics approximation is impractical at this date. However, the geometric parameters for all the cases including both experimental and numerical studies compared in this work are within the domain of validity of the one-dimensional geometric optics approximation. And since the two-dimensional geometric optics predictions agree well with all the existing approaches, it seems likely that the one-dimensional domain is valid for two-dimensional surfaces.

CONCLUSIONS

The geometric optics approximation is a ray tracing approach in which energy bundles are traced until they leave the surface. Its application to two-dimensional random rough surfaces has been studied. Geometric optics predictions have been compared with the findings from the few existing electromagnetic theory calculations and with the existing experimental findings from five experimental facilities. The examined cases include both metallic and dielectric materials with surface slopes ranging from 0.11–0.71. In general, the geometric optics predictions agree well with existing results and the comparisons indicate the capability of the geometric optics approximation to predict off-specular and retro-reflection peaks. Thus, the geometric optics approximation provides a useful and relatively inexpensive approach for the two-dimensional surface reflection for the cases with geometric parameters lying within the one-dimensional geometric optics domain of validity.

Acknowledgements—This research was supported, in part, by the National Science Foundation (NSF CTS 95-31772), the University of Illinois Research Board, Richard W. Kritzer Endowment Fund, Pittsburgh Supercomputing Center and the National Center for Supercomputing Applications. The authors thank Mr Y. Yang for his development of the two-dimensional surface generation code.

REFERENCES

1. Nieto-Vesperinas, M. and Sanchez-Gil, J. A., Light scattering from a random rough interface with total internal reflection. *Journal of the Optical Society of America A*, 1992, **9,** 424–436.
2. Nieto-Vesperinas, M. and Sanchez-Gil, J. A., Light transmission from a randomly rough dielectric diffuser: theoretical and experimental results. *Optical Letters*, 1990, **15,** 1261–1263.
3. Maradudin, A. A., Michel, T., McGurn, A. R. and Mendez, E. R., Enhanced backscattering of light from a random grating. *Annals of Physics*, 1990, **203,** 255–307.
4. Celli, V., Maradudin, A. A., Marvin, A. M. and McGurn, A. R., Some aspects of light scattering from a randomly rough metal surface. *Journal of the Optical Society of America A*, 1985, **2,** 2225–2239.
5. Soto-Crespo, J. M. and Nieto-Vesperinas, M., Electromagnetic scattering from very rough random surfaces and deep reflection gratings. *Journal of the Optical Society of America A*, 1989, **6,** 367–384.
6. Maradudin, A. A., Mendez, E. R. and Michel, T., Backscattering effects in the elastic scattering of *p*-polarized light from a large-amplitude random metallic grating. *Optical Letters*, 1989, **14,** 151–153.
7. Sanchez-Gil, J. A. and Nieto-Vesperinas, M., Light scattering from random dielectric surfaces. *Journal of the Optical Society of America A*, 1991, **8,** 1270–1286.
8. Dimenna, R. A. and Buckius, R. O., Electromagnetic theory predictions of the directional scattering from triangular surfaces. *ASME Journal of Heat Transfer*, 1994, **116,** 639–645.
9. Dimenna, R. A. and Buckius, R. O., Microgeometrical contour contributions to surface scattering. *Thermal Science and Engineering*, 1994, **2,** 166–171.
10. McGurn, A. P. and Maradudin, A. A., An analogue of enhanced backscattering in the transmission of light through a thin film with a randomly rough surface. *Optical Communications*, 1989, **72,** 279–285.

11. Gu, Z. H., Lu, J. Q., Martinez, A., Mendez, E. R. and Maradudin, A. A., Enhanced backscattering from a one-dimensional rough dielectric film on a glass substrate. *Optical Letters*, 1994, **19,** 604–606.
12. Gu, Z. H., Lu, J. Q., Maradudin, A. A. and Martinez, A., Enhanced backscattering from a free-standing dielectric film. *Applied Optics*, 1995, **34,** 3529–3534.
13. Maradudin, A. A., Lu, J. Q., Michel, T., Gu, Z. H., Dainty, J. C., Sant, A. J., Mendez, E. R. and Nieto-Vesperinas, M., Enhanced backscattering and transmission of light from random surfaces on semi-infinite substrates in thin films. *Waves in Random Media*, 1991, **3,** S129–S141.
14. Phu, P., Ishimaru, A. and Kuga, Y., Copolarized and cross-polarized enhanced backscattering from two-dimensional very rough surfaces at millimeter waves frequencies. *Radio Science*, 1994, **29,** 1275–1291.
15. Dimenna, R. A. and Buckius, R. O., Quantifying specular approximations for angular scattering from perfectly conducting random rough surfaces. *Journal of Thermophysics and Heat Transfer*, 1994, **8,** 393–399.
16. Tang, K., Dimenna, R. A. and Buckius, R. O., Regions of validity of the geometric optics approximation for angular scattering from very rough surfaces. *International Journal of Heat and Mass Transfer*, 1997, **40,** 49–59.
17. Tran, P. and Maradudin, A. A., The scattering of electromagnetic waves from a randomly rough 2D metallic surface. *Optical Communications*, 1994, **110,** 269–273.
18. Macaskill, C. and Kachoyan, B. J., Iterative approach for the numerical simulation of scattering from one- and two-dimensional rough surfaces. *Applied Optics*, 1993, **32,** 2839–2847.
19. Tsang, L., Chan, C. H. and Pak, K., Backscattering enhancement of a two-dimensional random rough surface (three-dimensional scattering) based on Monte Carlo simulations. *Journal of the Optical Society of America A*, 1994, **11,** 711–715.
20. Pak, K., Tsang, L., Chan, C. H. and Johnson, J., Backscattering enhancement of electromagnetic waves from two-dimensional perfectly conducting random rough surfaces based on Monte Carlo simulations. *Journal of the Optical Society of America A*, 1995, **12,** 2491–2499.
21. Johnson, J., Tsang, L., Shin, R. T., Pak, K., Chan, C. H., Ishimaru, A. and Kuga, Y., Backscattering enhancement of electromagnetic waves from two-dimensional perfectly conducting random rough surfaces: a comparison of Monte Carlo simulations with experimental data. *IEEE Transactions in Antennas and Propagation*, 1996, **44,** 748–755.
22. Tran, P., Celli, V. and Maradudin, A. A., Electromagnetic scattering from two-dimensional randomly rough, perfectly conducting surfaces: iterative methods. *Journal of the Optical Society of America A*, 1994, **11,** 1686–1689.
23. Tran, P. and Maradudin, A. A., Scattering of a scalar beam from a two-dimensional randomly rough hard wall: Dirichlet and Neumann boundary conditions. *Applied Optics*, 1993, **32,** 2848–2851.
24. Beckmann, P. and Spizzichino, A., *The Scattering of Electromagnetic Waves from Rough Surfaces*. Pergamon, 1963.
25. Thorsos, E., The validity of the Kirchhoff approximation for rough surface scattering using Gaussian roughness spectrum. *Journal of the Acoustical Society of America*, 1988, **83,** 78–92.
26. Chen, M. F. and Fund, A. K., A numerical study of the regions of validity of the Kirchhoff and small-perturbation rough surface scattering models. *Radio Science*, 1988, **23,** 163–170.
27. McCammon, D. F. and McDaniel, S. T., Surface reflection: on the convergence of a series solution to a modified Helmholtz integral equation and the validity of the Kirchhoff approximation. *Journal of the Optical Society of America A*, 1986, **79,** 64–70.
28. Liszka, E. G. and McCoy, J. J., Scattering at a rough boundary—extensions of the Kirchhoff approximation. *Journal of the Acoustical Society of America A*, 1982, **71,** 1093–1100.
29. Wirgin, A., Reflection from a corrugated surface. *Journal of the Acoustical Society of America*, 1980, **68,** 692–699.
30. He, X. D., Torrance, K. E., Sillion, F. X. and Greenberg, D. P., A comprehensive physical model for light reflection. *Computer Graphics*, 1992, **25,** 175–186.
31. Torrance, K. E. and Sparrow, E. M., Theory for off-specular reflection from roughened surfaces. *Journal of the Optical Society of America A*, 1967, **57,** 1105–1114.
32. Smith, A. M., Muller, P. R., Frost, W. and Hsia, H. M., Super- and subspecular maxima in the angular distribution of polarized radiation reflected from roughened dielectric surfaces. *Progress Astronautics and Aeronautics: Heat Transfer and Spacecraft Thermal Control*, ed. J. Lucas. AIAA, New York, 1971, pp. 249–269.
33. Ford, J. N., Tang, K. and Buckius, R. O., Fourier Transform Infrared system measurements of the bi-directional reflectivity of diffuse and grooved surfaces. *ASME Journal of Heat Transfer*, 1995, **117,** 995–962.
34. Arnold, C. B. and Beard, J. L., An ERIM perspective on BRDF measurement technology. *Proceedings SPIE*, 1989, **1165,** 112–135.
35. Dereniak, E. L., Stuhlinger, T. W. and Bartell, F. O., Bi-directional reflectance distribution function of gold-plated sandpaper. *Proceedings SPIE*, 1980, **257,** 184–191.
36. Knotts, M. E. and O'Donnell, K. A., Measurements of light scattering by a series of conducting surfaces with one-dimensional roughness. *Journal of the Optical Society of America A*, 1994, **11,** 697–710.
37. Smith, T. F., Suiter, R. L. and Kanayama, K., Bi-directional reflectance measurements for one-dimensional, randomly rough surfaces. *Progress in Astronautics and Aeronautics: Heat Transfer, Thermal Control, and Heat Pipes*, ed. W. Olstead. AIAA, New York, 1980, pp. 189–208.
38. Gu, Z. H., Dummer, R. S., Maradudin, A. A. and McGurn, A., Experimental study of the opposition effect in the scattering of light from a randomly rough metals surface. *Applied Optics*, 1989, **28,** 537–543.
39. Phu, P., Ishimaru, A. and Kuga, Y., Controlled millimeter-wave experiments and numerical simulations on the enhanced backscattering from one-dimensional very rough surface. *Radio Science*, 1993, **28,** 533–548.
40. Haner, D. A. and Menzies, R. T., Reflectance characteristics of reference materials used in lidar hard target calibration. *Applied Optics*, 1989, **28,** 857–864.
41. O'Donnell, K. A. and Mendez, E. R., Experimental study of scattering from characterized random surfaces. *Journal of the Optical Society of America A*, 1987, **4,** 1194–1205.
42. Gray, P. F., A method of forming optical diffusers of simple known statistical properties. *Optical Acta*, 1978, **25,** 765–775.
43. Chan, T. K., Kuga, Y., Ishimaru, A. and Le, C. T. C., Experimental studies of bistatic scattering from two-dimensional conducting random rough surfaces. *IEEE Transactions in Geoscience Remote Sensing*, 1996, **34,** 674–680.
44. Brewster, M. Q., *Thermal Radiative Transfer and Properties*, 1st edn. John Wiley and Sons, New York, 1992.
45. Modest, M. F., *Radiative Heat Transfer*. McGraw-Hill, New York, 1993.
46. Cohn, D. W., Tang, K. and Buckius, R. O., Comparison of theory and experiments for reflection from microcontoured surfaces. *International Journal of Heat and Mass Transfer*, 1997, **40,** 3223–3235.
47. TMA, Inc., Bi-directional reflectivity data for Spectralon™ and Infragold™ samples, Bozeman, MT, 1994.